JMEPEG (2007) 16:647–654
DOI: 10.1007/s11665-007-9092-5

1059-9495/$19.00

Understanding the Influence of Copper Nanoparticles on Thermal Characteristics and Microstructural Development of a Tin-Silver Solder

D.C. Lin, T.S. Srivatsan, G-X. Wang, and R. Kovacevic

(Submitted January 12, 2006; in revised form October 10, 2006)

This paper presents and discusses issues relevant to solidification of a chosen lead-free solder, the eutectic Sn-3.5%Ag, and its composite counterparts. Direct temperature recordings for the no-clean solder paste during the simulated reflow process revealed a significant amount of undercooling to occur prior to the initiation of solidification of the eutectic Sn-3.5%Ag solder, which is 6.5 °C, and for the composite counterparts, it is dependent on the percentage of copper nanopowder. Temperature recordings revealed the same temperature level of 221 °C for both melting (from solid to liquid) and final solidification (after recalescence) of the Sn-3.5%Ag solder. Addition of copper nanoparticles was observed to have no appreciable influence on melting temperature of the composite solder. However, it does influence solidification of the composite solder. The addition of 0.5 wt.% copper nanoparticles lowered the solidification temperature to 219.5 °C, while addition of 1.0 wt.% copper nanoparticles lowered the solidification temperature to 217.5 °C, which is close to the melting point of the ternary eutectic Sn-Ag-Cu solder alloy, Sn-3.7Ag-0.9Cu. This indicates the copper nanoparticles are completely dissolved in the eutectic Sn-3.5%Ag solder and precipitate as the Cu_6Sn_5, which reinforces the eutectic solder. Optical microscopy observations revealed the addition of 1.0 wt.% of copper nanoparticles to the Sn-3.5%Ag solder results in the formation and presence of the intermetallic compound Cu_6Sn_5. These particles are polygonal in morphology and dispersed randomly through the solder matrix. Addition of microsized copper particles cannot completely dissolve in the eutectic solder and projects a sunflower morphology with the solid copper particle surrounded by the Cu_6Sn_5 intermetallic compound coupled with residual porosity present in the solder sample. Microhardness measurements revealed the addition of copper nanopowder to the eutectic Sn-3.5%Ag solder resulted in higher hardness.

Keywords lead-free solder, nanoparticles, Sn-3.5%Ag, solidification, temperature recording

1. Introduction

One of the most extensively used joining techniques, namely soldering, has grown in stature to find enhanced application and use in the electronic industry. It has proven itself a technically sound and well-developed metallurgical joining method that essentially makes use of a specified filler material, which offers combinations of low melting point, good wetting characteristics and acceptable mechanical properties. As a joining material, the solder should have excellent dimensional stability coupled with good electrical, thermal, and even mechanical properties when put to use in electronic assemblies. The qualities of the solder itself coupled with the property of the interfaces between the solder and the substrate is critical to the overall integrity of a solder joint (Ref 1). For surface mount technology, especially in the optical and/or opto-electronic devices, solders having modified mechanical properties are desirable for applications that necessitate the need for reliability and dimensional stability (Ref 2, 3). In addition, technological requirements in the area of device packaging have provided the much-needed impetus to move beyond the domain of conventional solders.

An economically attractive and potentially viable method for enhancing the mechanical properties of a solder joint is to use particle-reinforced composite solders. The composite solder is obtained through: (a) the addition of reinforcing particles such as compounds of Cu_6Sn_5, TiO_2, FeSn, $FeSn_2$, and Ni_3Sn_2 to the solder, and (b) blending dissolvable particles, such as copper and nickel, with a conventional solder alloy to form in-situ intermetallic compounds (Ref 4-15). A variety of particulate reinforcements have been tried and used in an attempt to engineer a composite solder. Over the years, a large majority of the reinforcements used were either pure metal or intermetallic compounds with the particle size at the micron level. Researchers at the International Business Machines (IBM) Corporation developed composite solders by blending together: (a) powders of molybdenum (of average size of 200 meshes), or (b) powders of titanium (of average size of 200 meshes) with powders of the 50%Sn-50%Pb solder alloy. The resultant composite solder exhibited improved bonding strength with the metal substrate (Ref 7). Marshall and co-workers developed a composite solder by blending fine particles of the

D.C. Lin and **R. Kovacevic,** Research Center for Advanced Manufacturing, 3101 Dyer Street, Dallas, TX 75205; **T.S. Srivatsan** and **G-X. Wang,** Department of Mechanical Engineering, The University of Akron, 302 E. Buchtel Mall, Akron, OH 44325. Contact e-mail: tsrivatsan@uakron.edu.

intermetallic compound (Cu_6Sn_5) with a 60%Sn-40%Pb solder (Ref 9). Copper particles of size 8-microns and embedded in a Sn-Pb solder can enhance the creep-rupture lifetime of a soldered joint by an order of magnitude. This is attributed to the formation and presence of a thin layer of intermetallic compound between the reinforcing particle and the solder matrix, which was observed and reported by researchers at the Beijing University of Technology (Ref 10). The effect of adding copper particles and silver particles (with the average powder particle size of several microns) to a eutectic Sn-3.5%Ag solder on (a) microstructural development, (b) isothermal aging evaluation, and (c) creep response was studied by Guo et al. (Ref 11, 12). These researchers found that the creep resistance of the copper particle-reinforced eutectic Sn3.5%Ag solder was noticeably improved for the soldered joints at temperatures of 25, 65, and 105 °C. Earlier studies (Ref 13, 14) aimed at the development of high strength nanoparticle-reinforced composite solder have shown perfect mixing of the nano-sized ceramic titanium dioxide (TiO_2) and metallic copper in a Sn-37 Pb solder.

This paper presents the results of a research exercise aimed at understanding the influence of addition of copper nanopowders to a lead-free eutectic Sn-3.5%Ag solder in governing solidification response and microstructural development. In particular, the influence of addition of small weight percent of nanopowder to a eutectic Sn3.5%Ag solder on solidification characteristics and resultant microstructural development is examined and discussed.

2. Experimental Setup and Procedures

2.1 Selected Materials and Sample Preparation

Powders of a commercial high purity eutectic Sn-3.5%Ag solder paste having an average size of 45 μm (Fig. 1a), were thoroughly blended with nanopowders of pure copper having an average particle size 50 nm (Fig. 1b) to form a composite solder mixture. The Sn-3.5%Ag solder, in the no-clean form, was purchased from AIM Solder Corporation (Copley, Ohio, USA). The pure copper nanopowders were obtained from Invest-Technologies Company (Russia). Two different percentages of the copper powders, namely: (a) 0.5 wt.% copper, and (b) 1.0 wt.% copper, were chosen and used. The microsized copper powder having an average diameter in the range of 4-8 μm was purchased from Atlantic Equipment Engineers (Bergenfield, NJ, USA) and chosen for the purpose of comparison. The mechanical stirring was done for 30 min to ensure a near homogeneous distribution of the copper nanopowder in the solder mixture.

The well-mixed solder mixture (approximately 4 g in weight) was taken in two stainless steel crucibles, which were suspended from a shelf located within the furnace (experiment setup is shown in Fig. 2). The sample in one crucible was used for temperature recording, while sample in the other crucible was used for analyzing microstructure development and microhardness assuming no difference in the super-cooling behavior. To record temperature profile vs. time during the simulated reflow process, a J-type thermocouple (diameter = 0.127 mm and purchased from OMEGA ENGINEERING INC.) was placed inside the solder mixture. The recording system made use of the National Instrument Lab View 5.1 program encoded with FP-TC-120 modules. The samples were heated to prescribed limits within the temperature-controlled furnace. Both the heating rate and the high-temperature dwell time of the samples were controlled by presetting the furnace switch. The temperature readings for no-clean eutectic Sn-3.5%Ag solder is shown in Fig. 3(a), and the temperature readings for Sn-3.5%Ag solder containing copper nanoparticles is shown in Fig. 3(b).

To minimize the effects of sample oxidation commercial argon gas, with a flow rate of 4 L/min, was used as the shroud gas and allowed to flow freely over the surface of the sample. The cooling and resultant solidification of the sample takes place within the furnace with the power switched off. In this study, the average cooling rate was found to be 16 °C/min.

The as-solidified samples were thoroughly cleaned using aqueous hydrochloric acid solution to remove: (a) flux, (b) surface oxides, and (c) other contaminants on the sample surface. This was followed by ultrasonic cleaning of the solder samples in isopropanol followed by cooling by drying in ambient air.

2.2 Microstructural Characterization

The as-solidified samples were prepared using standard metallographic procedures for examination in an optical microscope under bright field illumination. The composition was measured by energy dispersive X-ray (EDX) analysis in a scanning electron microscope (SEM) to determine the following:

(a) The primary Sn-rich phase.
(b) The presence of the Ag_3Sn phase, and
(c) Presence of the Sn-Cu intermetallic compound.

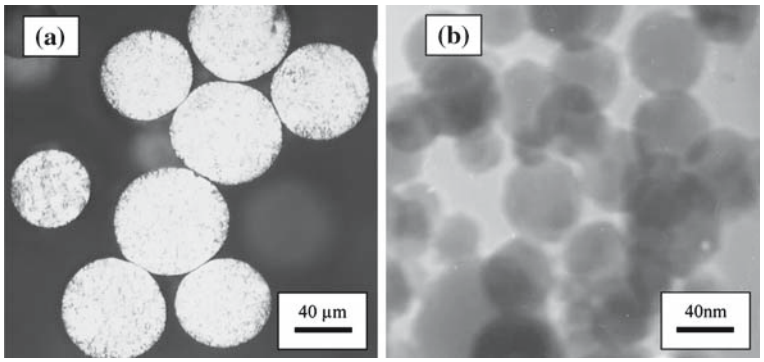

Fig. 1 Powder distribution used for this experiment. (a) Optical morphology to show Sn3.5%Ag alloy powder (45 μm in diameter). (b) TEM bright field image to show copper nanopowder (50 nm in diameter)

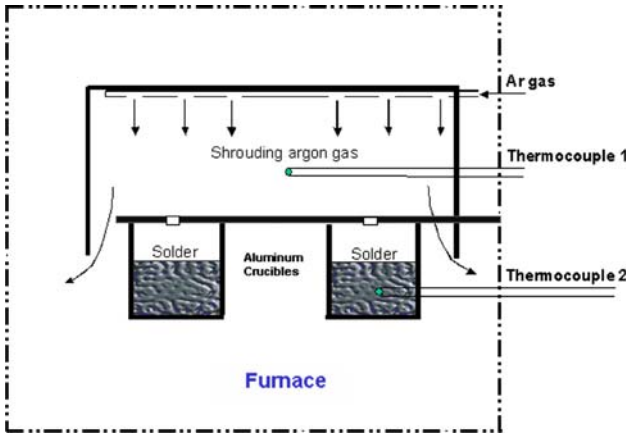

Fig. 2 Schematic of the experimental setup. The crucibles are of stainless steel with the thermocouple protected by a thin sheath

Even though accuracy of the EDX analysis is moderate, the results provide a reasonable map of the variation of tin, silver, and copper components in the sample.

Sample preparation initially involved cold sectioning followed by mounting in cold epoxy. This was followed by an initial coarse grind for removing the cutting layer and mechanically polished on progressively finer grades of silicon carbide impregnated emery paper using copious amounts of water as the lubricant. The samples were then fine polished using 3-µm and 1-µm alumina powder suspended in distilled water as the lubricant. Final polishing to near mirror-like surface finish was achieved using 0.3-µm and 0.05-µm diamond paste suspended in distilled water. The as-polished samples were chemically etched using a solution mixture of nitric acid (5 mL), hydrochloric acid (2 mL) and methanol (93 mL) for a few seconds. The etched surfaces of the solder samples were observed in an optical microscope with the objective of determining: (a) size and morphology of the grains, and (b) presence, distribution, and morphology of phases present in the microstructure.

2.3 Microhardness Testing

The value of hardness provides a measure of the resistance of the material to indentation, deformation, densification, and cracking. The Knoop microhardness (Hk) of the solder samples was measured using a Buehler Micromet II Microhardness tester. The indentation load used was 10 g. Higher loads can cause problems due to the following: (a) load dependence of hardness, and (b) promote the occurrence of localized microscopic cracking. To minimize the uncertainties from measurement and cracking of the as-consolidated composite solder samples, an indentation load of 10 g for a dwell time of 10 s was chosen. At least four indents were made on the polished surfaces of each sample, and the result is reported as the average value in units of kg/mm^2.

3. Results and Discussions

The primary objective of the present study was to explore the feasibility of using nanoparticles to reinforce a eutectic Sn3.5%Ag solder through in-situ formation of Cu_6Sn_5 particles. The focus being to establish the following:

(a) Thermal characteristics during cooling and solidification of the samples, which shows the influence of copper nanoparticles during cooling of the solder.
(b) The influence of nanoparticle addition on microstructural development.
(c) A comparison of the microhardness for different weight percentages of nanoparticles in the eutectic solder matrix.

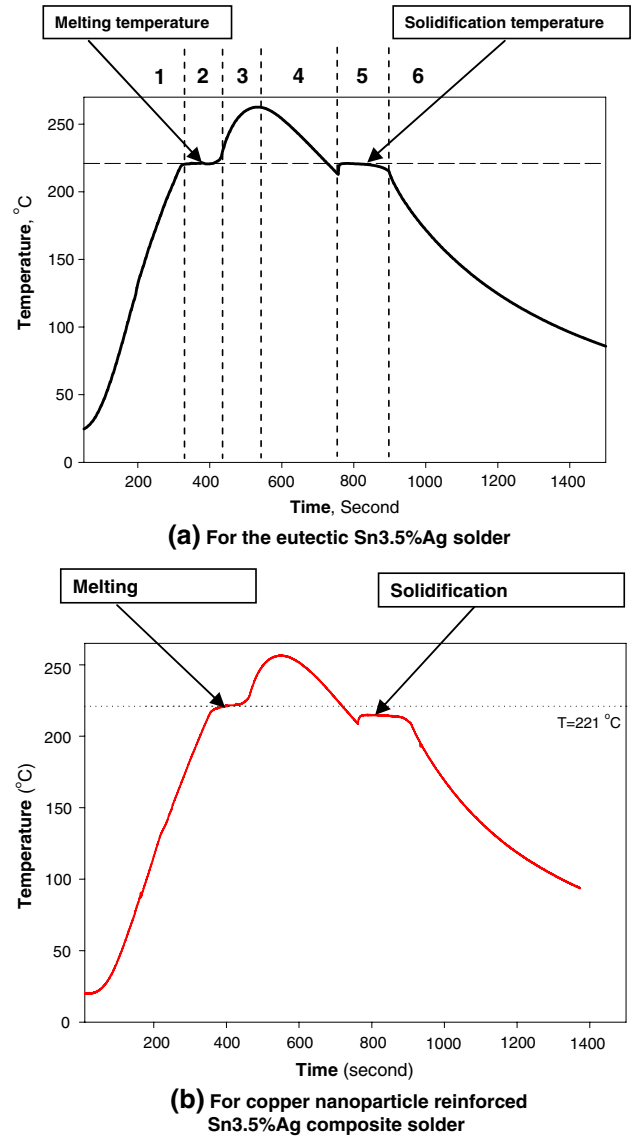

Fig. 3 Thermal histories of the solder samples during reflow process. (1) Heating stage from room temperature to melting temperature, (2) melting temperature, (3) molten state heating, (4) molten state cooling, (5) solidification from nucleation of grains to the end of solidifying, and (6) solid state cooling

3.1 Thermal Characteristics of Eutectic Sn3.5%Ag Solder

The thermal history of the eutectic Sn-3.5%Ag solder during the cycles of heating, melting, and cooling is shown in

Fig. 3(a). This figure provides a variation in temperature of the solder mixture (the solder powders surrounded by a chemical flux) with time. The entire process may be separated into six different sections. Area 1 in Fig. 3(a) shows the heating period from room temperature to melting point. A careful examination of this area reveals the heating rate to slightly change at temperatures around 130 °C. This is believed to be due to activation by the chemical flux. In this period, the heating rate is controlled and optimized because if the ramp in temperature is fast, then the solder mixture could explode outside of the container due to a rapid evaporation of the volatile paste carrier fluid resulting in the formation of spattered particle groups. Once the temperature reaches the melting point, initiation of melting occurs, coupled with a balanced competition between latent heat absorption and environmental heating to keep the measured temperature at about the same level. For the eutectic Sn3.5Ag solder, the melting temperature was found to be 221 °C from the binary phase diagram (Ref 16). This is confirmed in this study by the first plateau in Area 2 of Fig. 3(a).

The molten solder upon melting is continuously heated to a peak temperature of 250 °C (Area 3 in Fig. 3a). Cooling of the molten solder occurs when power to the furnace is turned off. The molten solder continues to cool to a temperature below the melting temperature (Area 4 of Fig. 3a). When the temperature reaches 214.5 °C for this eutectic Sn-3.5%Ag solder, initiation of nucleation occurs with the molten solder now starting to become solid. The solder sample is a mixture of mostly liquid with a small quantity of solid. Temperature of the solder mixture increases because of the latent heat that is released by the solidifying mass. This is followed by recalescence with the solder mixture being heated back to the equilibrium solidification temperature (Area 5 of Fig. 3a), which is representative of the competition between environment cooling occurring around the sample and the latent heat released by the solidifying solder. For the eutectic Sn-3.5%Ag solder, the equilibrium solidification temperature is the same as the melting temperature (221 °C as shown in Fig. 5 curve 1) and the degree of supercooling is around 6.5 °C (Fig. 4). Following recalescence there occurs continuous cooling of the solid solder to room temperature as shown by Area 6 of Fig. 3(a).

3.1.1 The Influence of Copper Nanoparticle on Thermal Characteristics of Eutectic Sn-3.5%Ag solders. Regarding the addition of copper nanoparticles to the eutectic solder, it was noticed that the melting temperature of the Sn-3.5% solder paste mixture was not appreciably affected by the presence of trace amount of copper nanoparticles, an example is Fig. 3(b). The melting point is around 221 °C. However, addition of copper nanopowder does affect the molten composite solder. Influence of percentage of copper nanopowder addition on solidification temperature of the Sn-3.5%Ag alloy is shown in Fig. 3(b) and for purpose of comparison in Fig. 5 (curves 1-3). Addition of 0.5 wt.% copper nanopowder, curve 2 in Fig. 5 reveals the solidification temperature to be 219.5 °C with a supercooling of 9.5 °C. For the addition of 1.0 wt.% copper nanopowder, curve 3 in Fig. 5 reveals the solidification temperature to be 217.5 °C with the super-cooling drop to around 5 °C.

The solidification temperature is affected by the addition of copper nanoparticles because of a reaction of the powder particles with tin. Once powders of the solder and the surrounding flux become molten, the dissolution of copper particles is facilitated by a reaction of the copper nanopowder

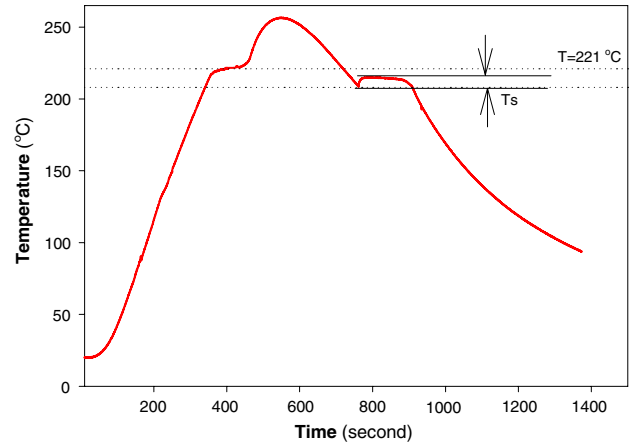

Fig. 4 Schematic of the measurement of degree of supercooling (Ts)

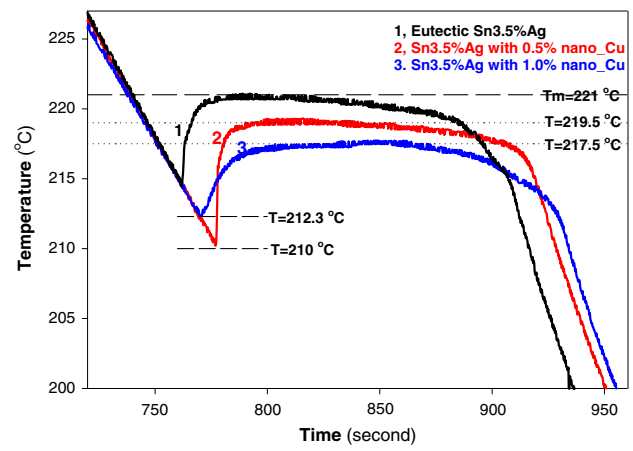

Fig. 5 Comparison of super-cooling for the Copper nanoparticle-reinforced Sn-3.5Ag solder. Nucleation temperature of the Sn3.5Ag eutectic is at 214.5°C

with the Sn-based solder. As a result, the solder melt becomes locally a Sn-Ag-Cu ternary alloy with co-existence of the Sn-Ag binary system. The resultant molten composite solder is a mixture of the eutectic Sn-3.5%Ag and the ternary Sn-Ag-Cu alloy surrounding the powder particles of copper. Figure 5 suggests that the copper nanopowders are completely dissolved in the molten Sn3.5%Ag solder during the melting process for the 0.5 and 1.0 wt.% at the solidification temperature when compared to the eutectic Sn-Ag-Cu composition (Ref 17). A similar thermal history, as shown in Fig. 3(b), was obtained by Chada et al. (Ref 18) during the reflow process of a eutectic Sn-Ag solder spread on a copper substrate.

3.2 Microstructure of the Eutectic Sn-Ag Solder

The microstructure of the bulk eutectic Sn-3.5%Ag solder at a cooling rate of 16 °C/min was thoroughly examined and a cross section is shown in Fig. 6 at (a) low magnification (Fig. 6a) to visualize the overall morphology, and (b) higher magnification (Fig. 6b) to observe the distribution of second-phase particles. At the lower magnification, two distinct regions were identified for the eutectic Sn-dominant solder. The white

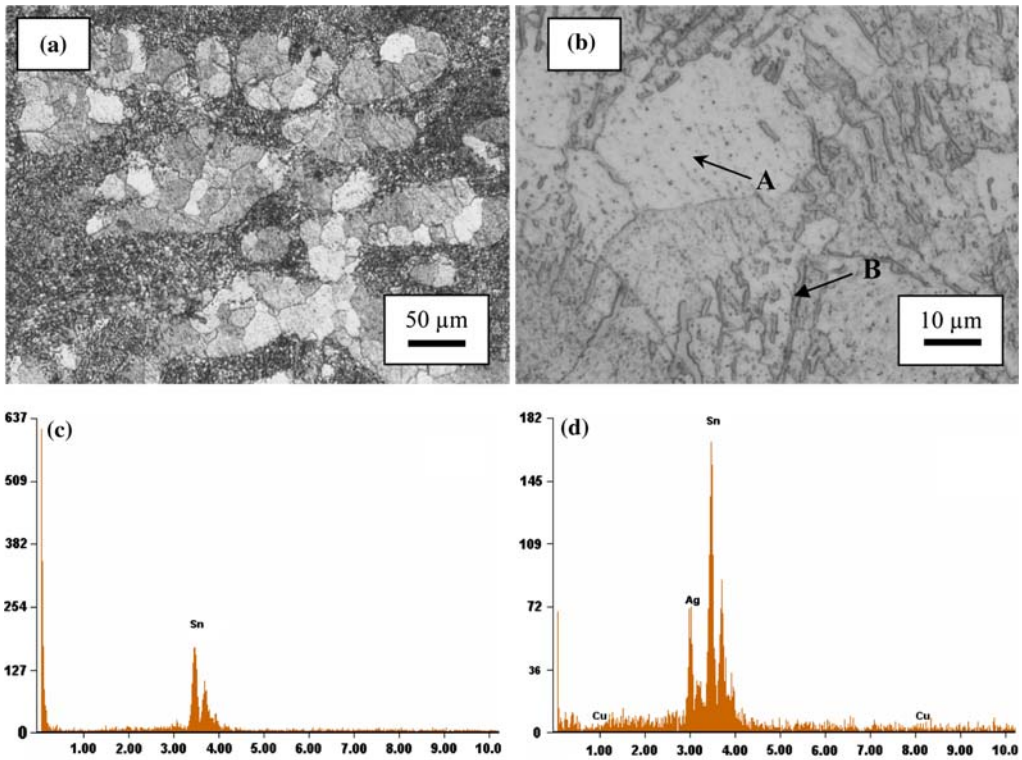

Fig. 6 Optical microstructure and its companion identification in an SEM of the eutectic Sn-3.5%Ag solder. (a) Lower magnification to show the overall microstructure, (b) higher magnification to show the detail information, (c) EDS analysis of phase A at image (b) to show Sn-dominant phase (d) element distribution for phase B at image (b)

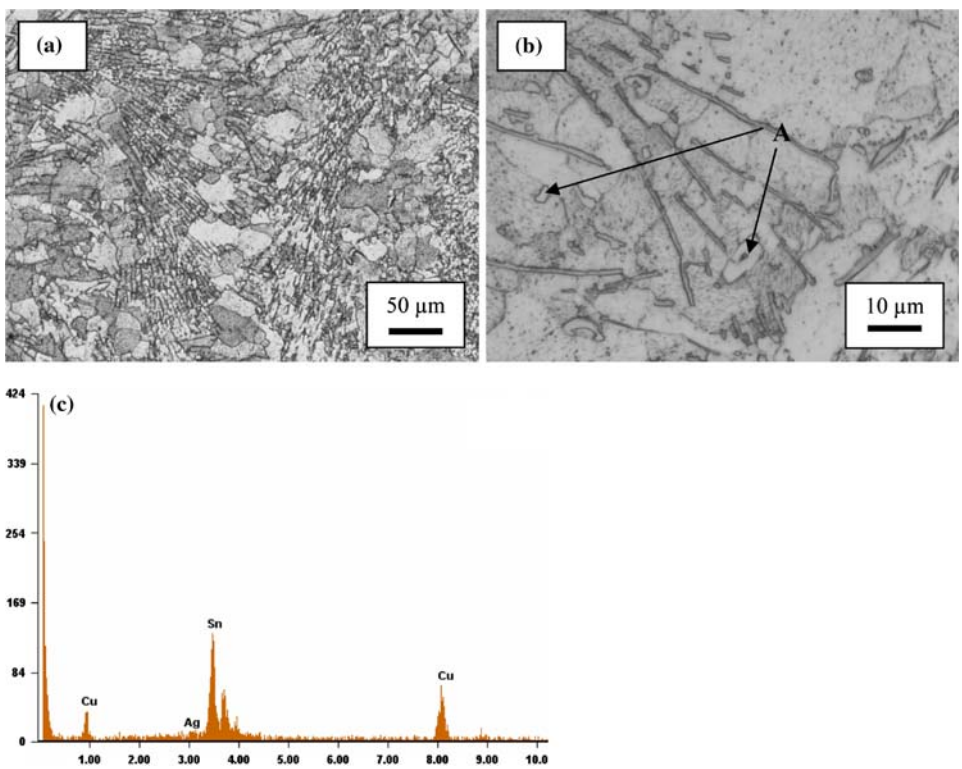

Fig. 7 Optical microstructure and companion identification of the Sn-3.5%Ag solder containing 0.5% copper nanopowder. (a) Lower magnification to show the overall microstructure, (b) higher magnification to show the detail information, and (c) EDS analysis for phase A at image (b) to show Sn-Cu compound

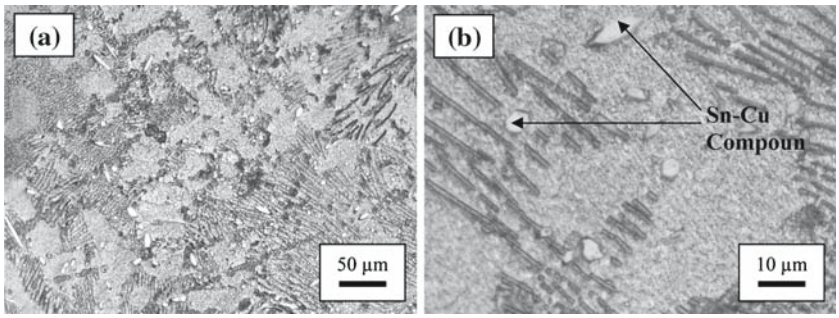

Fig. 8 Optical microstructure of Sn-3.5%Ag solder with 1.0% copper nanopowder. (a) Lower magnification to show the overall microstructure and (b) higher magnification to show the detail information

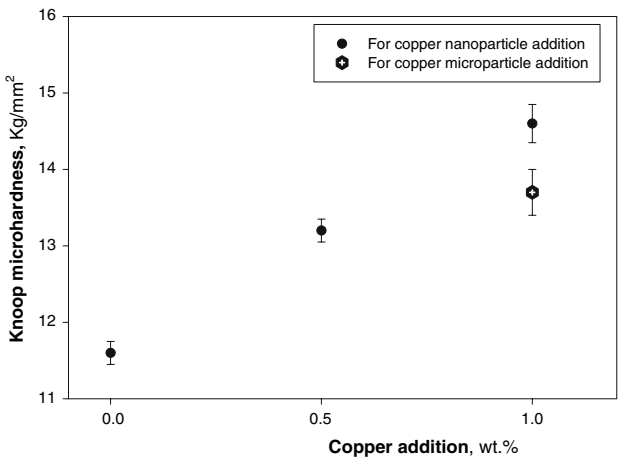

Fig. 9 Knoop microhardness of Sn-3.5%Ag with various Cu additions

phase is the primary Sn-rich phase, marked as A in Fig. 6(b). An EDS analysis of this phase is shown in Fig. 6(c) and the element distribution is 100% Sn. The dark region is the compound Ag_3Sn and marked as B in Fig. 6(b). An EDS analysis of this phase is shown in Fig. 6(d). At higher magnifications, the micrograph reveals the light colored regions, representing the tin-rich phase, and the dark-colored regions, representing the Ag_3Sn phase. This microstructure appears mainly to be eutectic with the Sn-rich primary phase fairly well distributed in a Sn-rich phase/Ag_3Sn eutectic. A similar structure was observed by others for this type of eutectic solder for varying levels of the cooling rate (Ref 11, 12, 19).

3.3 Effect of Copper Nanoparticles on Microstructure of the Eutectic Sn-3.5%Ag Solder

Addition of copper nanopowder has an influence on thermal characteristics as shown in Fig. 5. Further, it also influences microstructural development as is evident in the optical microscopy observations of the Sn-3.5%Ag solder containing 0.5 wt.% copper nanopowder and shown in Fig. 7. The addition of copper nanopowder did not appreciably influence the formation, presence, and morphology of the Ag_3Sn phase, which has a needle-like morphology. However, the nanopowder refines the Sn-rich structure and the number of distinct and separate Sn-rich islands is much more than in the eutectic structure. Addition of copper nanopowders promotes the formation and presence of the Sn-Cu intermetallic. The second-phase intermetallic compound was near polygon in shape and identified by EDS (Fig. 7c). This intermetallic compound was identified in an earlier study to be the Cu_6Sn_5 (Ref 20). The microstructure of the eutectic Sn3.5%Ag solder containing 0.5% Cu powder consists of three distinct phases: (a) the Sn-rich phase, (b) Ag_3Sn phase, and (c) the intermetallic compound Cu_6Sn_5.

For 1.0 wt.% copper nanopowder addition, the Cu_6Sn_5 intermetallic compound was found to be fairly well distributed through the solder matrix (Fig. 8). Comparing with microstructure of the eutectic Sn3.5%Ag solder (Fig. 6), the morphology of the primary Sn-rich phase is refined and more uniformly distributed through the solder matrix, and the Ag_3Sn needles were interrupted by the presence of the Cu_6Sn_5 phase (Fig. 8b). The increase in Cu_6Sn_5 content is responsible for the observed increase in hardness from 11.8 kg/mm^2 for the eutectic Sn-3.5%Ag solder to 13.2 kg/mm^2 for the Sn-3.5%Ag containing 0.5 wt.% Cu nanopowder to 14.6 kg/mm^2 for the Sn3.5%Ag containing 1.0 wt.% Cu nanopowder (Fig. 9). The microhardness of the composite solder increases by 20% through the in-situ precipitation of the compound Cu_6Sn_5.

For purpose of comparison, the microstructure of the Sn3.5%Ag composite solder containing 1.0 wt.% micron-sized copper powder (4-8 μm) was obtained under identical reflow process as shown in Fig. 10. The existence of un-melted or undissolved copper powder was observed at the center of sunflower morphology and identified by an EDS analysis (Fig. 10c) to be pure copper. The sunflower morphology is located on top of the solder sample, suggesting its migration from the matrix to the top during melting. Subramanian and Lee (Ref 21) also observed the sunflower morphology. Its microhardness (Fig. 9) is noticeably lower than the counterpart containing copper nanopowder. This clearly indicates that even though the micron-sized copper powders can reinforce the eutectic Sn-3.5%Ag solder, the difference in the amount and distribution of intermetallic compounds limits its performance. The micron-sized copper particles migrate to the top of the solder on account of their lower ductility with respect to the surrounding molten solder.

4. Conclusions

Based on a study of the influence of copper nanopowder on thermal characteristics and microstructural development of a eutectic Sn-3.5%Ag solder, the following are the key findings.

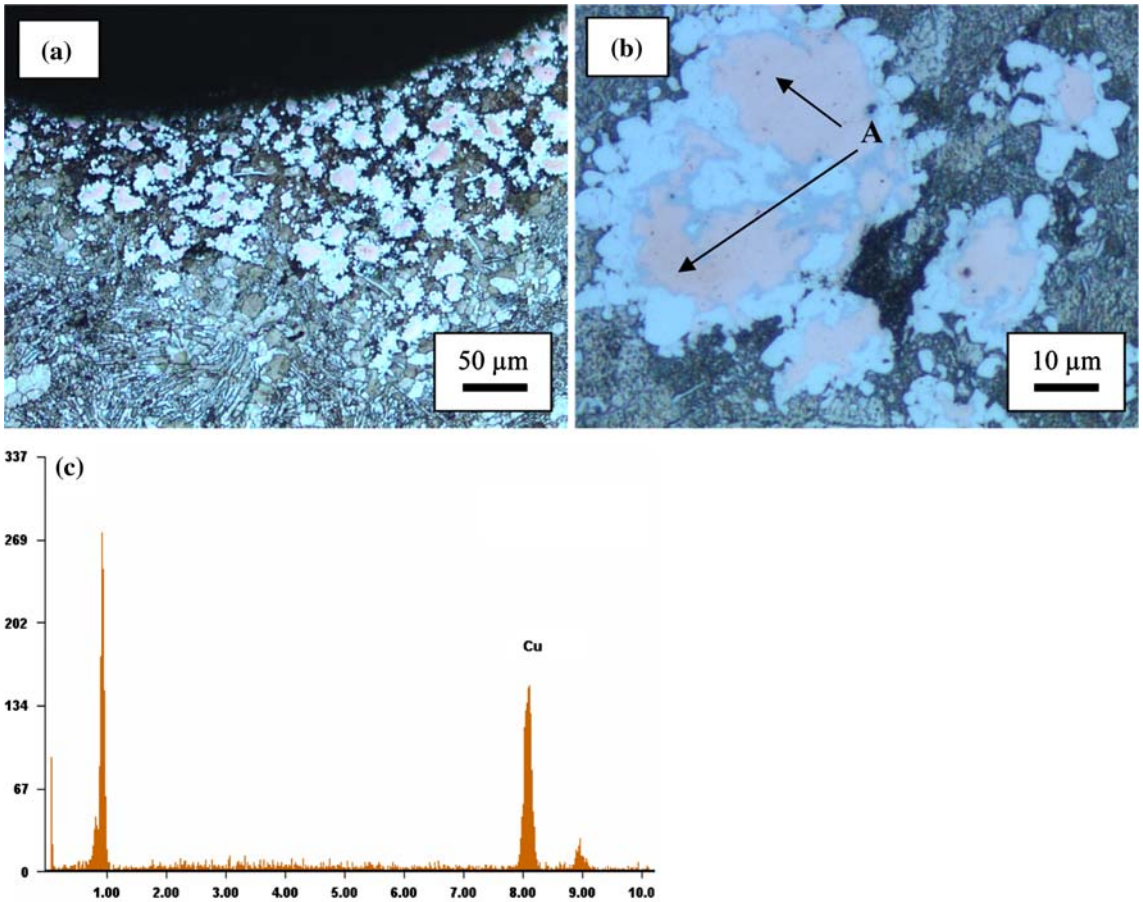

Fig. 10 Optical microstructure of Sn-3.5%Ag solder with 1.0% copper micropowder. (a) Lower magnification to show the overall microstructure, (b) higher magnification to show the detail information, and (c) EDS analysis for phase A at image (b) to show nondissolved copper

(a) Experiments were successfully conducted to carefully examine the solidification characteristics and microstructural development of a eutectic Sn-3.5%Ag solder reinforced with in-situ Cu_6Sn_5 compound through blending with nano-sized powders of copper.
(b) Thermal history of the Sn-3.5%Ag solder mixture containing copper nanopowder is characterized by melt undercooling followed by isothermal solidification at a lower solidification temperature.
(c) The addition of copper nanopowder refines the tin-rich primary phase while concurrently ensuring a uniform distribution of the intermetallic compound (Cu_6Sn_5) through the solder matrix. This results in an increase in microhardness by up to 20%.

Acknowledgments

This research work was jointly supported by: (a) the NER Grant from National Science Foundation (DMI-0103159), (b) Firestone Research Initiative Fellowship, (c) Summer Faculty Research Grant of University of Akron, and (d) Research Fellowship from Research Center for Advanced Manufacturing in Southern Methodist University. Sincere thanks and appreciation is extended to the unknown reviewers for their critical comments and suggestions which have helped strengthen this technical manuscript.

References

1. J.H. Lau, *Solder Joint Reliability: Theory and Applications*. Van Nostrand Reinhold, New York, p 1–30
2. P.A. Bouleau, Packaging for Optoelectronic Interconnections, *J. Metals*, 1994, **46**(6), p 41–45
3. H. Mavoori, Dimensionally Stable Solders for Optoelectronics and Microelectronics, *J. Metals*, 2000, **52**, p 29–32
4. J.L. Marshall and J. Calderon, Hard-particle Reinforced Composite Solders Part 1: Micro-characterisation, *Solder. Surface Mount Technol.*, 1997, **26**, p 22–28
5. Y. Wu, J.A. Sees, C. Pouraghabagher, L.A. Foster, J.L. Marshall, E.G. Jacobs, and R.F. Pinizzotto, The Formation and Growth of Intermetallic In Composite Solder, *J. Electron. Mater.*, 1993, **22**(7), p 769–777
6. J.H. Lee, D.J. Park, J.N. Heo, Y.H. Lee, D.H. Shin, and Y.S. Kim, Reflow Characteristics of Sn-Ag Matrix In-situ Composite Solders, *Scripta Mater.*, 2000, **42**(8), p 827–831
7. Composite Solders, IBM Technical Disclosure Bulletin, vol. 29(4), 1986, p 1573–1574
8. I. Dutta, B.S. Majumdar, D. Pan, W.S. Horton, W. Wright, and Z.X. Wang, Development of a Novel Adaptive Lead-Free Solder Containing Reinforcements Displaying the Shape-Memory Effect, *J. Electron. Mater.*, **33**(4), p 258–270
9. J.L. Marshall, J. Calderon, J. Sees, G. Lucey, and J.S. Hwang, Composite Solders, *IEEE Trans. Components Hybrids Manufact. Technol.*, 1991, **14**(4), p 698–702
10. Y.F. Yan, J.P. Liu, Y.W. Shi, and Z.D. Xia, Study on Cu Particles-enhanced SnPb Composite Solder, *J. Electron. Mater.*, 2004, **33**(3), p 218–225
11. F. Guo, S. Choi, J.P. Lucas, and K.N. Subramanian, Microstructural Characterisation of Reflowed and Isothermally-aged Cu and Ag

Particulate Reinforced Sn-3.5Ag Composite Solders, *Solder. Surface Mount Technol.*, 2001, **13**(1), p 7–18

12. F. Guo, J.P. Lucas, and K.N. Subramanian, Creep Behavior in Cu and Ag Particle-reinforced Composite and Eutectic Sn3.5%Ag and Sn4Ag0.5Cu non-composite Solder Joints, *J. Mater. Sci. Electron.*, 2001, **12**, p 27–35
13. D.C. Lin, G.X. Wang, T.S. Srivatsan, M. Al-Hajri, and M. Petraroli, Influence of Titanium Dioxide Nanopowder Addition on Microstructural Development and Hardness of Tin–Lead Solder, *Mater. Lett.*, 2003, **57**, p 3193–3198
14. D.C. Lin, S. Liu, T.M. Guo, G.-X. Wang, T.S. Srivatsan, and M. Petraroli, An Investigation of Nanoparticles Addition on Solidification Kinetics and Microstructure Development of Tin-Lead Solders, *Mater. Sci. Eng. A*, 2003, **360**, p 285–292
15. S. Choi, J.P. Lucas, K.N. Subramanian, and T.R. Bieler, Formation and Growth of Interfacial Intermetallic Layers in Eutectic Sn-Ag Solder and its Composite Solder Joints, *J. Mater. Sci.: Mater. Electron.*, 2000, **11**(6), p 497–502
16. H. Okamoto, *Phase Diagrams of Dilute Binary Alloys*. ASM International, Materials Park, OH, 2002, p 241
17. K.W. Moon, W.J. Boettinger, U.R. Kattner, F.S. Biancaniello, and C.A. Handwerker, Experimental and Thermodynamic Assessment of Sn-Ag-Cu Solder Alloys, *J. Electron. Mater.*, 2000, **29**(10), p 1122–1136
18. S. Chada, A. Herrmann, W. Laub, R. Fournelle, D. Shan guan, and A. Achari, Microstructural Investigation of Sn-Ag and Sn-Pb-Ag Solder Joints, *Solder. Surface Mount Technol.*, 1997, **9**, p 9–13
19. F. Ochoa, J.J. Williams, and N. Chawla, The Effects of Cooing Rate on Microstructure and Mechanical Behavior of Sn-3.5%Ag Solder, *J. Metals*, 2003, June, p 56–60
20. M. S. G.W. H.S. McCormack Jin Kammlott Chen, New Pb-free Solder Alloy with Superior Mechanical Properties, *Appl. Phys. Lett.*, 1993, **63**, p 15–17
21. K.N. Subramanian and J.G. Lee, Physical Metallurgy in Lead-free Electronic Solder Development, *J. Metals*, 2003, May, p 26–32